# AtlantECO

Atlantic Ecosystems Assessment, Forecasting & Sustainability

# Deliverable number 6.1 - Dataset of ocean reanalysis and hindcast simulation version 1

## Dissemination level: Public

| | |
|---|---|
| Related Work Package | WP6 Advances in model predictability |
| Related task(s) | Task 6.1 |
| Lead beneficiary | CMCC |
| Author(s) | D. Iovino, P.G. Fogli, S. Masina (CMCC) |
| Due date | 28.02.2022 |
| Submission date | 24.02.2022 |
| Type | Report |
| Status and version | Final, v1.0 |

**Declaration:** *Any work or result described therein is a genuine output of the AtlantECO project. Any other source will be properly referenced where and when relevant.*

## Table of Content

# 1   Version History

| Version | Authors | Summary of changes | Date |
|---------|---------|--------------------|------|
| 0.1 | D. Iovino, P.G. Fogli | Initial draft | 21/02/2022 |
| 0.2 | S. Masina | internal review | 24/02/2022 |
| 0.3 | M. Vichi | Review | 25/02/2022 |
| 0.4 | E. van Seville | Review | 25/02/2022 |
| 1.0 | D. Iovino, P.G. Fogli | Final version | 25/02/2022 |
| 1.0 | D. Iudicone | Review for submission | 28/02/2022 |

## 2   Executive summary

The Deliverable "Dataset of ocean reanalysis and hindcast simulation version 1" is produced as part of the Work Package 6 "Advances in model predictability". It describes the multi-year ocean-sea ice simulation at 1/16° horizontal resolution and 98 vertical levels, whose 3D daily fields were provided in the  upper 540m of the whole Atlantic ocean (including the Nordic Seas) for the decade 2009-2018, within Subtask 6.1.1.
One variable for one time record is stored per file in CF-compliant NetCDF4 (lossless compression) for a total size of 12 Tb. The dataset is available upon registration through the CMCC Data Delivery System (DDS) at https://dds.cmcc.it/#/dataset/glob16-atlantic-ocean and it is identified by the following digital object identifier doi: 10.25424/cmcc/glob16-atlantic-2021

*This document is based on the terms and conditions established in the Grant Agreement (GA) and its Annexes, as well as in the Consortium Agreement (CA).*

# 3   Introduction

The AtlantECO Project aims to assess and predict changes in the status and dynamics of Atlantic Ocean ecosystems at regional and basin scales to improve the sustainability of ecosystem services. Work Package 6 "Advances in model predictability" focuses on the availability and use of high resolution and realistic simulations of the ocean dynamics/ecosystems. Predictability is a fundamental requirement for models that are employed as instruments for forecasting the ocean dynamics, and for predicting climate variability and climate changes at global or regional scales. Toward a comprehensive assessment of ecosystem structures and functions in the context of ocean circulation at multiple scales, one major challenge is in describing the fine-scale ocean processes and connecting them with (micro)biological functioning at regional and basin scales.

To properly resolve and predict the connectivity of water and organic matters within and between biogeographic regions and to resolve physical drivers at multiple scales, a combination of Eulerian and Lagrangian formulations is used in WP6, the former to describe the oceanic fields and their variability in time from large to fine scales, and the latter to describe the trajectories of parcels and their content in the ocean. This combination allows us to know what time scales and through which pathways, water flows from different locations and by geographic regions in the Atlantic and with that how water pollutants, plastic, plankton and other organisms are transported.

Within the last decades, computing power has become sufficient to make mesoscale-rich resolution affordable in the ocean and sea-ice models over the global system, which allows the ocean model to simulate more intense internal variability than a lower resolution model.

The Euro-Mediterranean Center on Climate Change (CMCC) contributes to Task 6.1 providing a high-resolution simulation of the daily-average dynamics of the three-dimensional Atlantic Ocean. This report describes the global eddying configuration of the ocean and sea ice system, the experimental design, and presents an overview of the GLOB16 performances to highlight the effect of eddying resolution.

# 4   Model configuration and experimental design

The CMCC simulation of the ocean-sea ice system is based on the Ocean Model Intercomparison Project (OMIP, Griffies et al., 2016), endorsed by the phase 6 of the World Climate Research Programme (WCRP) Coupled Model Intercomparison Project (CMIP6; Eyring et al., 2016).

It was organized by the Ocean Model Development Panel (OMDP) of the WCRP core program Climate and Ocean Variability, Predictability, and Change (CLIVAR), and proposed as support to the development and analysis of global ocean–sea-ice models used as a component of the Earth System models participating in CMIP6 (Griffies et al., 2016). The essential element behind the OMIP is a common set of atmospheric and river runoff datasets for computing surface boundary fluxes to drive the ocean–sea-ice models. The phase 2 of OMIP makes use of a surface-atmospheric dataset, JRA55-do version 1.4 (Tsujino et al., 2018), suitable for ocean and sea-ice models based on the Japanese 55-year Reanalysis and river runoff. The JRA55-do forcing has a 3-hour temporal resolution and a ~0.5° horizontal resolution. The turbulent heat and momentum fluxes of JRA55-do data have been computed using the bulk formula of Large and Yeager (2004).

The continental river discharge is provided by a river-routing model forced by river runoff from the land-surface component of JRA-55, and incorporates discharge of ice-sheets and glaciers from Greenland (Bamber et al., 2018) and Antarctica (Depoorter et al., 2013).

The experiment follows the OMIP-2 protocol, with the initial condition of the temperature and salinity given by the World Ocean Atlas 2013 observed fields WOA13v2 (Locarnini et al., 2013; Zweng et al., 2013), and a state of rest.

An evaluation of no-eddying ocean simulations from CMIP6-class global ocean–sea-ice models is presented in Tsujino et al. (2020), while the robustness of climate-relevant improvements in ocean simulations (mean and variability) associated with eddy-resolving (~0.1°) horizontal resolutions is assessed by Chassignet et al. 2020. A 61-year (1958–2018) global eddy-rich simulation for phase 2 of the Ocean Model Intercomparison Project has been produced by the global ocean-sea ice system GLOB16 (Iovino et al., 2016), developed at CMCC, and based on version 3.6 of the state-of-the-art NEMO ocean model (Madec and the NEMO team, 2016), coupled to the Louvain-la-Neuve sea Ice Model (LIM2, Fichefet and Morales Maqueda, 1997). GLOB16 makes use of a nonuniform tripolar grid for both ocean and sea ice, following the semi-analytical method of Madec and Imbard (1996). The horizontal grid has a 1/16° resolution at the Equator, corresponding to 6.9 km, that increases poleward as cosine of latitude (~4km at 60°N), leading to 5762 × 3963 grid points horizontally. The vertical coordinate system is based on fixed depth levels and consists of 98 vertical levels with a grid spacing increasing from approximately 1 m near the surface to 160 m in the deep ocean.

The GLOB16 bathymetry is generated from three distinct topographic products: ETOPO2 (US Department of Commerce, 2006) is used for the deep ocean, GEBCO (IOC, IHO and BODC, 2003) for the continental shelves shallower than 300 m, and Bedmap2 (Fretwell et al., 2013) for the Antarctic region, south of 60∘S. Bottom topography is represented as partial steps (Barnier et al., 2006).

OMIP2-GLOB16 was run on the global 3D ocean domain scale for one cycle of the atmospheric reanalysis from Jan 1958 to December 2018. The simulation produced monthly-averaged 3D ocean state for the entire period of integration and daily-averaged ocean state from the last 10 years, from Jan 2009. In the framework of Task 6.1, CMCC provided the daily-averaged ocean temperature, salinity, zonal, meridional and vertical components of the ocean velocity for the entire Atlantic Ocean. The domain is set by a rectangular box that extends from 98°W to 21°E and from the Antarctic coastline to the northern boundary of the Nordic Seas (~79°N), in a depth range of 540 m (first 50 vertical levels) from the ocean surface. It is worth mentioning that the Atlantic box was cut from the native grid of the ocean model, a global orthogonal curvilinear mesh, rather than a regular geographic grid.

To identify the robust improvements associated with high horizontal resolution given the same forcing datasets, we also configured an eddy-permitting ocean-sea ice model, hereafter called ORCA205, which has an horizontal mesh at 1/4° with 75 vertical levels. This simulation is based on the same NEMO ocean component, similar physical parameters, and follows the same experimental protocol.

# 5   Model time evolution and drift

In this section, we present a set of basic large-scale diagnostics for assessing the relative quality, variability, and sensitivity of eddy-rich versus eddy-permitting ocean simulations. We use key metrics common in climate modelling, here applied to the global domain and the Atlantic Sector.
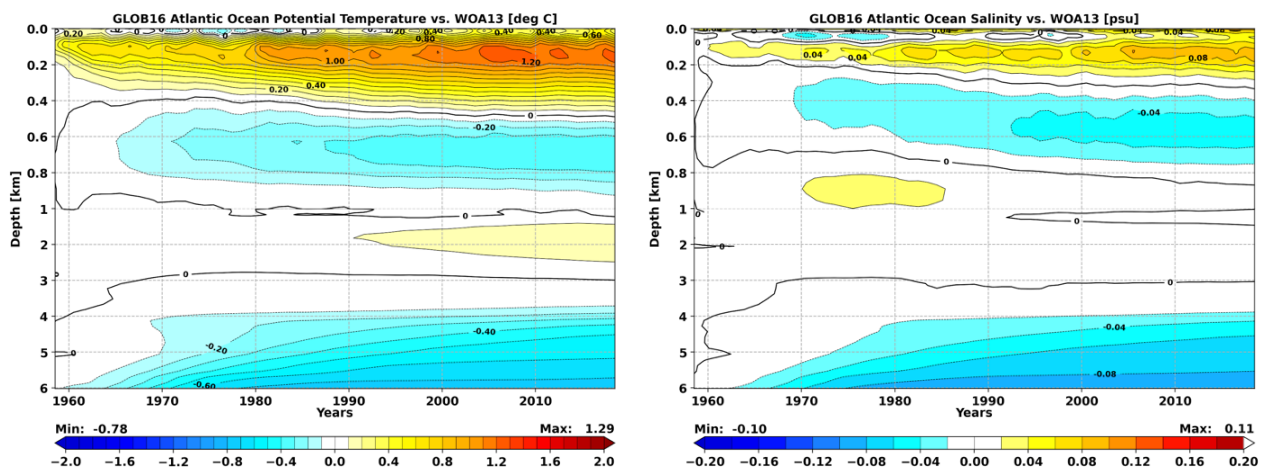
## 5.1   Temperature and salinity

First, we present the time evolution of the globally-averaged (potential) temperature and salinity. The drifts of annual-mean temperature and salinity are depicted vertically-averaged in the upper 500 m, in Figure 1. Upper-ocean temperature increases relative to the initial year, and GLOB16 warms faster than the lower-resolution ocean. Salinity presents only small changes with an overall freshening, slightly weaker in GLOB16. Because of the compensation between the upper and deeper layers, the temperature and salinity averaged over all depths change only slightly. The time evolution in each of the major ocean basins mimics that of the global domain. In particular, the time evolution of the GLOB16 Atlantic temperature and salinity from the initial condition as a function of depth is presented in Figure 2. The Atlantic basin becomes warmer and more saline in the upper layer, accompanied by a cooling and freshening of the deep ocean. The upper Atlantic warming is limited to ~100 m at the beginning of the integration, increases up to 1°C and deepens down to ~400 m. There is a salinification  (up to 0.08 psu) in the upper 200 m compensated by a freshening in

the deeper Atlantic ocean. Model drifts are mainly due to the adjustment of the simulation from the initial WOA conditions towards the new state imposed by the surface forcing (the same in the two simulations), but initial drifts evolve also due to parameter choices, and structural biases where the model is not able to correctly represent the dynamics of the real ocean due to limitations in grid resolution or parameterisations. It is worth mentioning that WOA13v2 has a resolution of 1/4°, coarser than GLOB16, and does not include fine scale details like the narrow current systems close to continental boundaries.
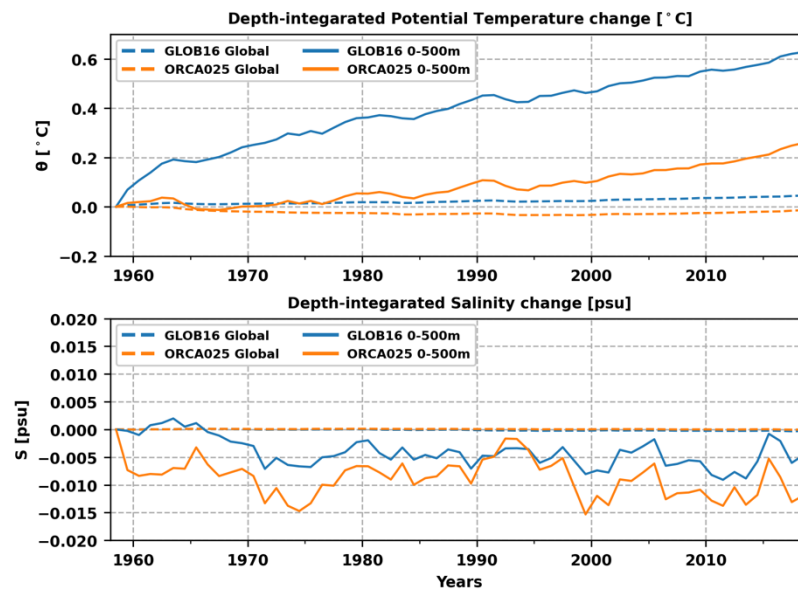


*Figure 1. Time evolution of global temperature (°C) and salinity (psu) change (relative to initial conditions) vertically averaged in the upper 500m (solid lines) and in the full depth (dashed lines), for GLOB16 (blue) and ORCA025 (orange).*



*Figure 2. Time evolution of the Atlantic Ocean temperature (°C) and salinity (psu) changes as a function of depth for GLOB16.*

The drift plots indicate that temperature and salinity bias structures are well established within the first decades of integration, so that time averages computed over the last decade of the simulations provide a reasonable estimate of the stationary bias characteristics of the model. Figure 3 shows latitude-longitude maps of surface temperature and salinity biases in the Atlantic Sector, computed over the final 10 years (from 2009 to 2018) with respect to the climatology used for the initialization. The changes in horizontal and vertical resolution significantly modify the vertical drift structure in both temperature and salinity - ORCA025 shows cooling and persistent salinification between 200 m and 1000 m (not shown).
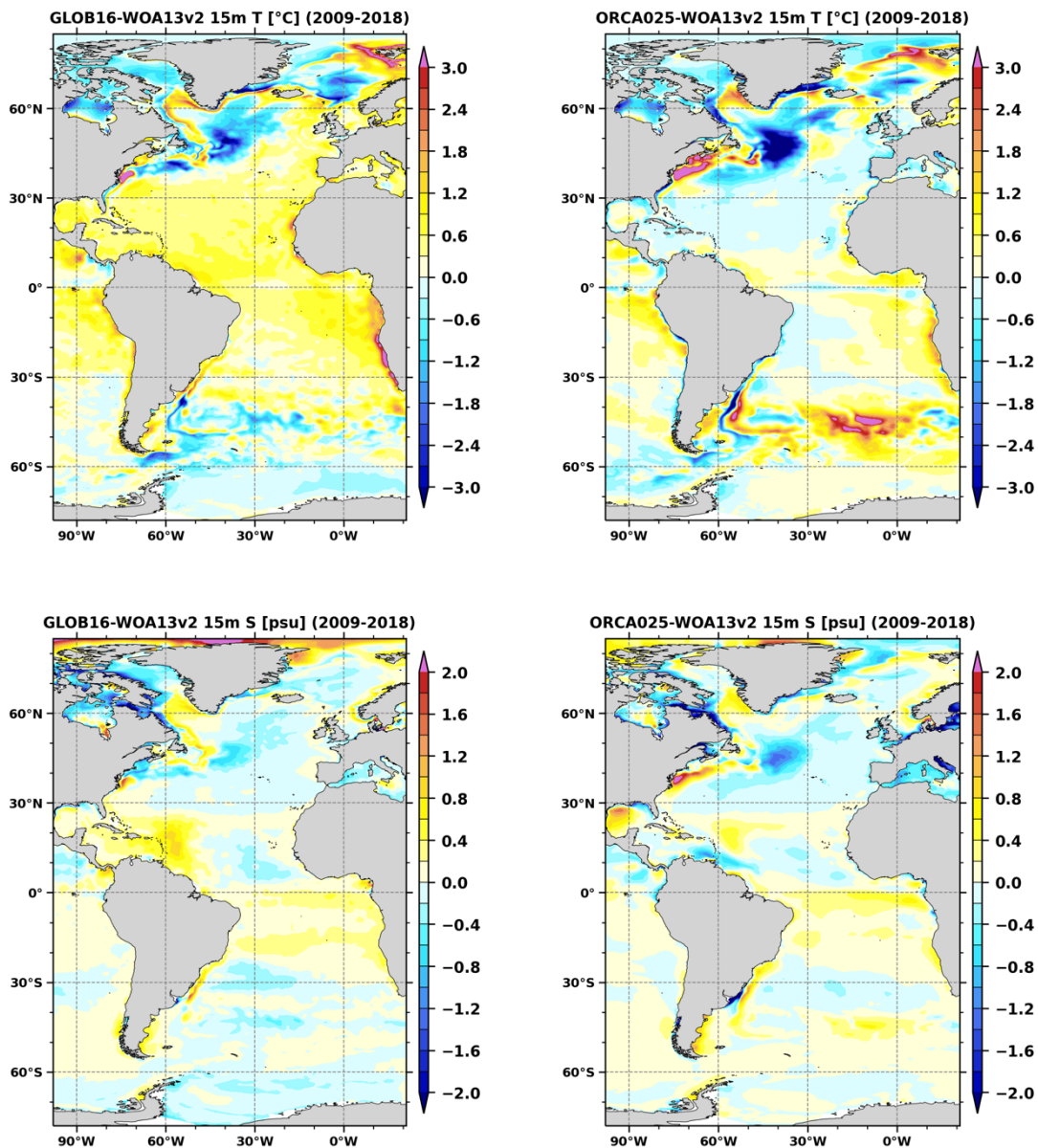


*Figure 3.* *Differences between mean 10-year (2009-2018) temperature (°C) and salinity (psu) at 15m relative to WOA13v2 climatology used to initialize the model for GLOB16 (left) and ORCA025 (right).*

The overall bias patterns of Atlantic temperature and salinity at the surface (15 m) are consistent between the two simulations. Beside a larger warming in the tropical and mid-latitude bands, and cooling in the Antarctic region, the most significant difference arising with the eddying resolution is in the subpolar region with a

significant reduction of magnitude and spatial distribution of the "North Atlantic cold bias" off Newfoundland. This cold bias is associated with a too zonal path of the North Atlantic Current and a missing northwest branch, typical of non-eddying and eddy-permitting ocean models. The cold bias is present also in GLOB16 but is less severe and more spatially confined. The ability of GLOB16 in resolving smaller scale features and currents results in a more realistic pathway of the circulation in the upper Atlantic Ocean, which increases the transport of heat and salt toward the Labrador Sea. Both models exhibit a warm and salty bias along the US coast around 40°N. Both biases persist along the Gulf Stream path in the lower resolution model while in GLOB16 the SST and SSS positive biases tend to disappear.

## 5.2   Kinetic energy

The spin-up of the circulation, as measured by the total kinetic energy (KE) and its eddy component (EKE) averaged over the whole domain (Figure 4), demonstrates the extent to which a quasi-steady state has been reached at the end of the simulation. The time evolution of the domain-averaged kinetic energy of the system [defined as 0.5 $(u^2 + v^2)$, where u and v are the 1-month averages of the horizontal velocity components] is very similar between configurations from 1958 to 2018. Both exhibit a quick spin-up of the kinetic energy in the first two years which levels off for the rest of the integration.
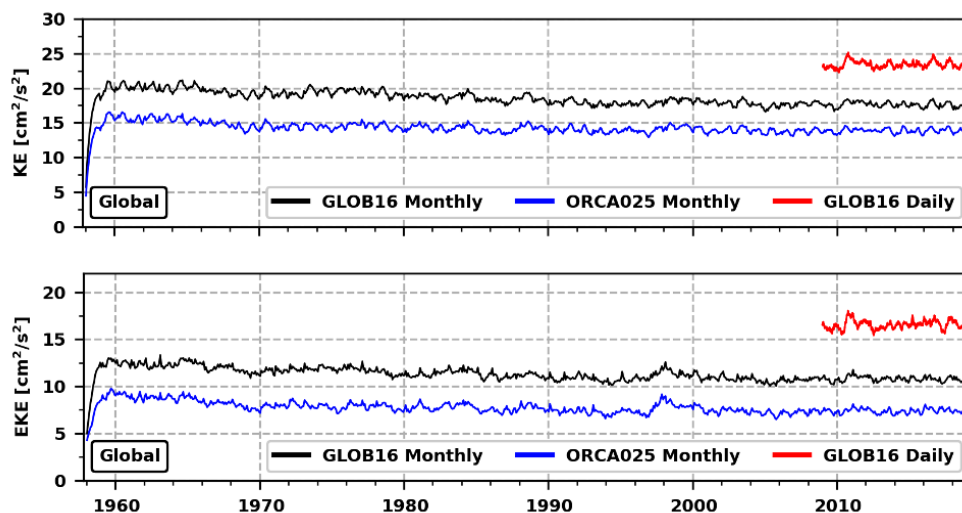


**Figure 4.** *Time evolution of the global domain-averaged kinetic energy (cm$^2$/s$^2$) for both experiments. Monthly-mean output is used for the long-term variability (black and blue lines), daily-mean for the last decade (red lines).*

Not surprisingly, the total kinetic energy is significantly higher for GLOB16 over ORCA25, but remains significantly lower than what can be inferred from observations and even higher-resolution models (e.g. Chassignet and Xu, 2017). Most of the kinetic energy is in the eddy field: the mean GLOB16 EKE (computed as the deviation of monthly velocity fields from the long-term mean velocities) contributes ~60% to the total basin-averaged budget. It is worth noting the impact of the method of calculation on the resulting budget: there is a significant increase in KE and EKE when computing them using 1-day average outputs (red lines as opposed to the monthly frequency in black), with the largest effect being on the eddy component that increases by ~30%. The time averaging removes much of the small-scale variability associated with inertial motions and ageostrophic effects. This suggests a reduction in the modeled energy when computing it by post-processing model outputs as opposed to online computation at every time step.

The eddy kinetic energy evolution for the Atlantic Ocean is displayed for GLOB16 at 15m and 250m in Figure 5 and is decomposed between the Northern and Southern ocean. At the surface, the North Atlantic contribution dominates with a well-pronounced seasonal cycle: EKE increases by ~30% from winter to the highest values in summer/autumn. The North Atlantic EKE presents a positive tendency in the last years of integration that is not reproduced in the Southern Ocean, which shows less variability. The EKE in the two hemispheres is comparable at 250m with the Southern Ocean that tends to regulate the basin-scale seasonal and interannual variability.

As horizontal resolution increases in GLOB16, the non-linearity of the solution allows for a better representation of western boundary currents, eddies form through barotropic and baroclinic instabilities over most of the Atlantic Ocean where the first Rossby radius of deformation is resolved (Hallberg, 2013). The eddy kinetic energy maps for both models are compared to estimates from the Copernicus-GlobCurrent surface ocean currents product (Rio, 2015), which provides geostrophic and Ekman currents at 15m depth on 3-hourly bases,on a regular 1/4° grid.
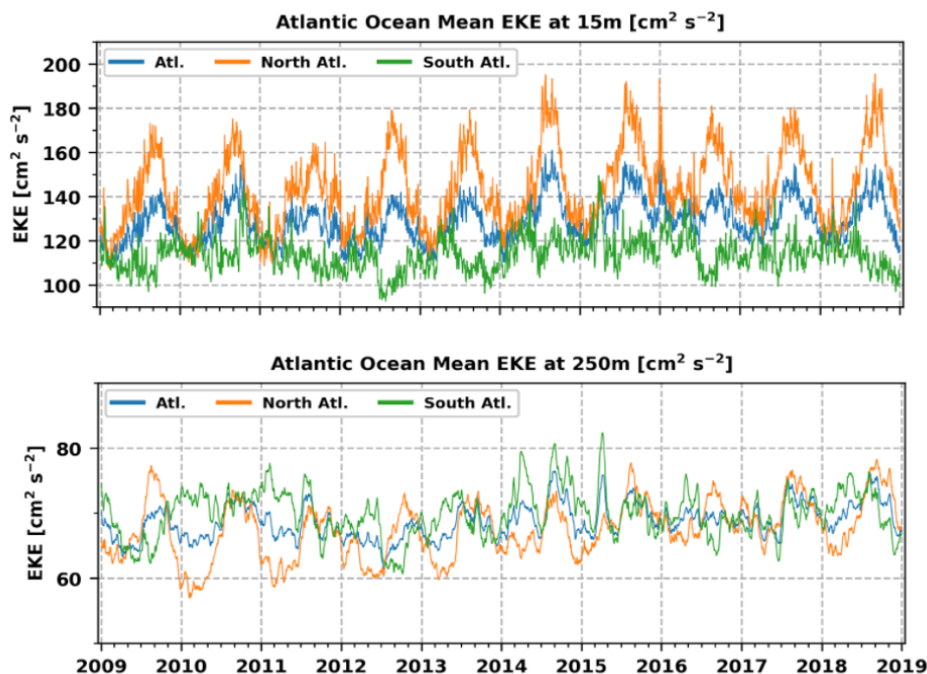


**Figure 5.** *Time evolution of the 15 m (top panel) and 250m (bottom panel) Atlantic-averaged eddy kinetic energy ($cm^2/s^2$) for the last decade of integration, computed from daily velocity fields.*

The GLOB16 spatial distribution agrees with observation-based estimates, with GLOB16 EKE generally lower in the tropical and subtropical regions. GLOB16 properly reproduces the energetic surface flow in the northwestern basin with an EKE of ~1000 $cm^2/s^2$ and largely improves the eddy dynamics in the Antarctic Circumpolar Current. It is worth noting that while GlobCurrent is more eddy-energetic at middle latitudes (in particular in the Gulf Stream region and gyres interior), it misrepresents the surface ocean circulation in the Labrador Sea and Nordic Seas where the energetic boundary currents are absent.
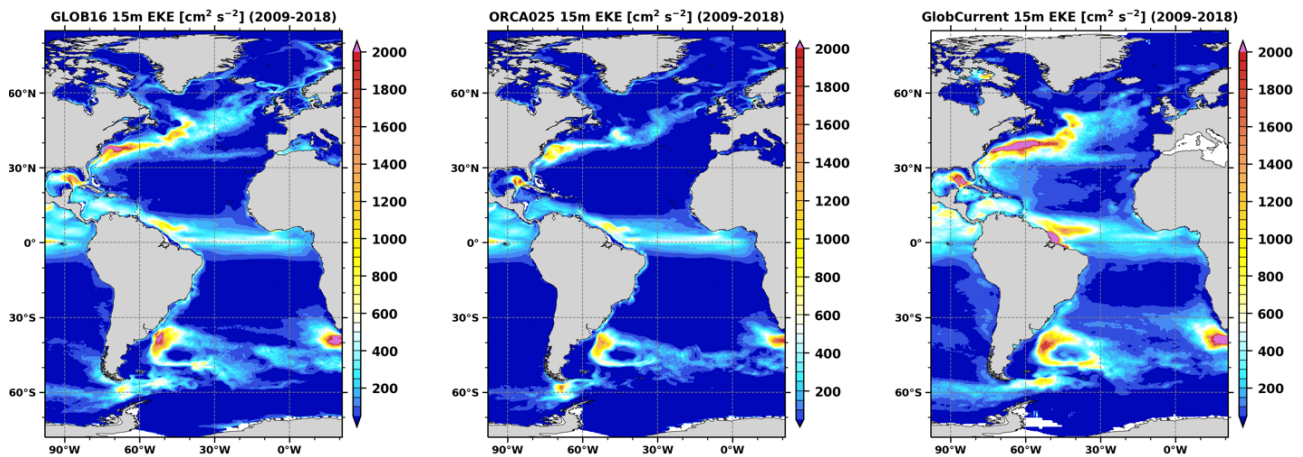
**Figure 6.** *Time-mean average of the eddy kinetic energy (cm²/s²) at 15 m from 1-day average fields averaged in the last decade of integration for GLOB16, ORCA025 and the GlobCurrent product.*

The accurate representation of the narrow boundary current in these regions is of high relevance in simulating the climate system. Eddies generated from these boundary currents are crucial to control the stratification within the regions, exporting their properties towards the center of the basins. With a focus on the Labrador Sea, we highlight the changes produced in the strength of stratification by resolving mesoscale (50 to 500 km) processes. The convective energy (here defined as the amount of energy needed to produce a neutrally stratified column extending down to a reference depth of 2000 m) is presented for GLOB16 and ORCA025 in Figure 7. With fewer and larger eddies resolved, the ORCA025 interior remains very weakly stratified across a wide region. In GLOB16, with more mesoscale features and stronger eddy fluxes from the Greenland coast, the convective energy is higher, and the spatial extent of the weakly stratified region has shrunk and is limited within the interior of the Labrador Sea, as opposed to ORCA025 where it spills out of the basin. The reduction of convective area (and volume) as resolution increases largely impacts the formation of dense water in the basin.
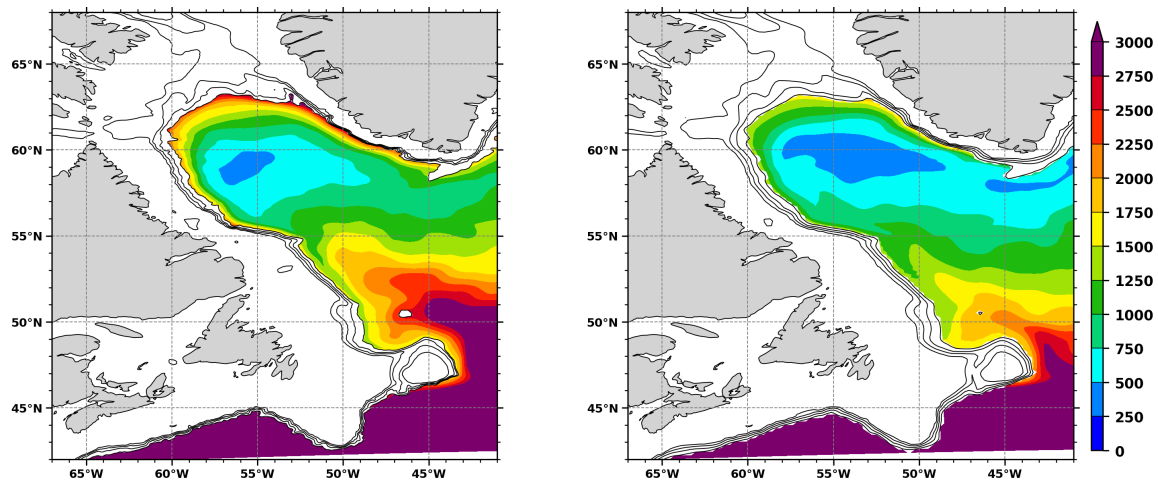


**Figure 7.** *Convective energy (J/m3) down to 2000 m, averaged from 2009 to 2018, for GLOB16 (right) and ORCA025 (left). Bathymetric lines (in black) are shown from 0 to 2000m with 500m contour interval.*

# 6   Data availability

The dataset provided in Task 6.1 consists of daily-mean fields of potential temperature, salinity, horizontal and vertical components of sea water velocity in the upper 540 meters of the Atlantic Ocean. The data set covers the last 10 years (2009-2018) of a 61-year hindcast simulation performed with the CMCC ocean-sea ice system at eddying resolution. The Atlantic region is defined as a rectangular box (1903 x 3896 horizontal grid points and 50 vertical geopotential levels) from 98°W to 21°E and from the Antarctic coastline up to the Nordic Seas (included in the domain). Model output files are available in the Climate and Forecast (CF)-compliant NetCDF4 format (with lossless compression) format. Each file consists of a CF header with a set of components (variables, dimensions, data type, units, content description, missing value and global attributes) and the data section that contains the actual values. Each file stores one 3D variable for one time record, for a total size of 12 Tb.

The dataset is available through the CMCC Data Delivery System (DDS, https://dds.cmcc.it/) that provides a seamless access point for all data produced and used by CMCC through a unified API interface. The screenshot of the DDS home page is in Figure 8 with a set of model outputs, publicly available. The Atlantic Ocean outputs requires registration to be directly found at https://dds.cmcc.it/#/dataset/glob16-atlantic-ocean. It is identified by the following digital object identifier doi: 10.25424/cmcc/glob16-atlantic-2021 .
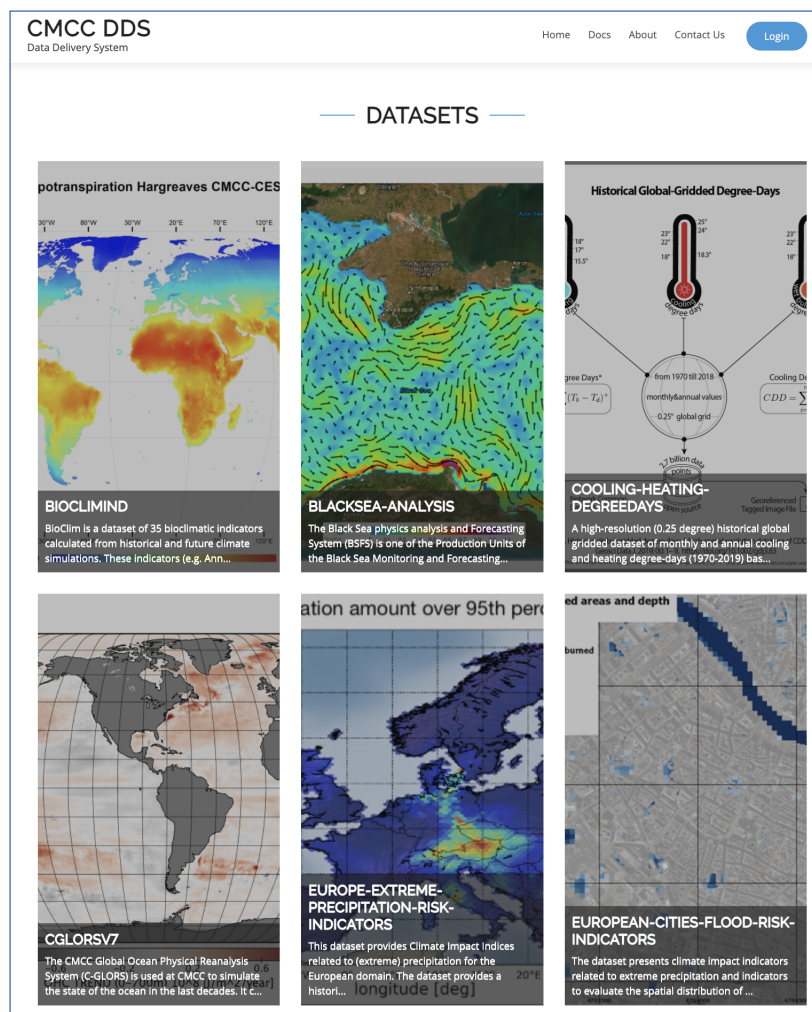


*Figure 8. The CMCC Data Delivery System home page, https://dds.cmcc.it/*

Any registered user can access and download data through the DDS Python Application Program Interface (API) client, available through Anaconda or the Python Package Index (PyPI). Example showing how to use the DDS API are at https://dds.cmcc.it/#/docs.

The command lines in Figure 9 are a sample data script in Python to manage the frequency of the model output download (files for one day at a time).

```python
import datetime   as dt
import ddsapi

# Initialize the client
c = ddsapi.Client()

# Dataset DDS id
dsid = "glob16-atlantic-ocean"

# Query dataset infos
ret = c.datasets(dsid)
if (ret["status"]!="OK"):
    raise RuntimeError("No such dataset available in the DDS repository: "+dsid)

# Download daily data, 1 day at a time
variables = ["thetao", "so", "uo", "vo", "wo"]
years = range(2009, 2019) # 2009-2018
months = range(1, 13) # 1-12
dpm = (31, 29, 31, 30, 31, 30, 31, 31, 30, 31, 30, 31)
#
for var in variables:
    for year in years:
        for month in months:
            for day in range(1, dpm[month]+1):
                #
                # Leap day check
                if (month==2):
                    try:
                        dt.datetime(year=year, month=month, day=day)
                    except:
                        continue
                #
                # retrieve data
                ret = c.retrieve(dsid,
                    {
                        "product_type": "daily",
                        "variable": [ var ],
                        "time": {
                            "year": [ year, ],
                            "month": [ month, ],
                            "day": [ day, ]
                        },
                        "format": "netcdf"
                    },
                    target="GLOB16_1d_{:s}_{:04d}{:02d}{:02d}.nc".format(var, year,
month, day))
```

*Figure 9. Python script to manage data download (examples are provided also on the data set webpage).*

# 7   Conclusion

The overall goal of this report is to provide a general description of the CMCC eddying ocean-sea ice system, GLOB16, present an overview from the whole 61-year global simulation but with a focus on the 2009-2018 decade, and finally assess the accuracy of the configuration in reproducing the ocean properties and circulation in the Atlantic Ocean. We used a set of large-scale diagnostics for assessing the relative quality and variability of GLOB16 versus a low-resolution ocean. GLOB16 shows good skill in reproducing the ocean average state and in representing the variability in the upper ocean. The gain due to explicitly resolving mesoscale dynamics in the entire Atlantic domain is evident when compared to a coarser-resolution version of the model. Gross characteristics of the bias and near-surface EKE patterns are significantly improved in the eddying ocean. However, the GLOB16 upper ocean warms more quickly than ORCA025, suggesting possible improvement in the parameterizations of vertical eddy heat transport. We have used the Labrador Sea region, as a key region in Atlantic climate studies, to stress how strongly mesoscale processes can regulate variability and structure of the 3D ocean dynamics, governing the overall water stratification.

# 8   Table of figures

**Figure 1.** Time evolution of global temperature (°C) and salinity (psu) change (relative to initial conditions) vertically averaged in the upper 500m (solid lines) and in the full depth (dashed lines), for GLOB16 (blue) and ORCA025 (orange).

**Figure 2.** Time evolution of the Atlantic Ocean temperature (°C) and salinity (psu) changes as a function of depth for GLOB16.

**Figure 3.** Differences between mean 10-year (2009-2018) temperature (°C) and salinity (psu) at 15m relative to WOA13v2 climatology used to initialize the model for GLOB16 (left) and ORCA025 (right).

**Figure 4.** Time evolution of the global domain-averaged kinetic energy ($cm^2/s^2$) for both experiments. Monthly-mean output is used for the long-term variability (black and blue lines), daily-mean for the last decade (red lines).

**Figure 5.** Time evolution of the Atlantic-averaged eddy kinetic energy ($cm^2/s^2$) for the last decade of integration, computed from daily velocity fields.

**Figure 6.** Time-mean average of the eddy kinetic energy ($cm^2/s^2$) at 15 m from 1-day average fields averaged in the last decade of integration for GLOB16, ORCA025 and the GlobCurrent product.

**Figure 7.** Convective energy (J/m3) down to 2000 m, averaged from 2009 to 2018, for GLOB16 (right) and ORCA025 (left). Bathymetric lines (in black) are shown from 0 to 2000m with 500m contour interval.

**Figure 8**. The CMCC Data Delivery System home page, https://dds.cmcc.it/

**Figure 9**. Python script to manage data download (examples are provided also on the data set webpage).

# 9   References

Bamber, J. L., Tedstone, A. J., King, M. D., Howat, I. M., Enderlin, E. M., van den Broeke, M. R., and Noel, B.: Land ice freshwater budget of the Arctic and North Atlantic Oceans: 1. Data, methods, and results, J. Geophys. Res.-Oceans, 123, 1827–1837, https://doi.org/10.1002/2017JC013605, 2018.

Barnier, B., Madec, G., Penduff, T., Molines, J. M., Treguier, A. M., Le Sommer, J., Beckmann, A., Biastoch, A., Boning, C., Dengg, J., Derval, C., Durand, E., Gulev, S., Remy, E., Talandier, C., Theetten, S., Maltrud, M.,

McClean, J., and De Cuevas, B.: Impact of partial steps and momentum advection schemes in a global ocean circulation model at eddy permitting resolution, Ocean Dynam., 56, 543–567, 2006.

Chassignet, E. P., Yeager, S. G., Fox-Kemper, B., Bozec, A., Castruccio, F., Danabasoglu, G., Horvat, C., Kim, W. M., Koldunov, N., Li, Y., Lin, P., Liu, H., Sein, D. V., Sidorenko, D., Wang, Q., and Xu, X.: Impact of horizontal resolution on global ocean–sea ice model simulations based on the experimental protocols of the Ocean Model Intercomparison Project phase 2 (OMIP-2), Geosci. Model Dev., 13, 4595–4637, https://doi.org/10.5194/gmd-13-4595-2020, 2020.

Chassignet, E. P. and Xu, X.: Impact of horizontal resolution ($1/12°$ to $1/50°$) on Gulf Stream separation, penetration, and variability, J. Phys. Oceanogr., 47, 1999–2021, https://doi.org/10.1175/JPOD-17-0031.1, 2017.

Depoorter, M. A., Bamber, J. L., Griggs, J. A., Lenaerts, J. T. M., Ligtenberg, S. R. M., Van Den Broeke, M. R., and Moholdt, G.: Calving fluxes and basal melt rates of Antarctic ice shelves, Nature, 502, 89–92, https://doi.org/10.1038/nature12567, 2013.

Eyring, V., Bony, S., Meehl, G. A., Senior, C. A., Stevens, B., Stouffer, R. J., and Taylor, K. E.: Overview of the Coupled Model Intercomparison Project Phase 6 (CMIP6) experimental design and organization, Geosci. Model Dev., 9, 1937–1958, https://doi.org/10.5194/gmd-9-1937-2016, 2016.

Fichefet, T. and Morales Maqueda, M. A.: Sensitivity of a global sea ice model to the treatment of ice thermodynamics and dynamics, J. Geophys. Res., 102, 12609–12646, 1997.

Fretwell, P., Pritchard, H. D., Vaughan, D. G., Bamber, J. L., Barrand, N. E., Bell, R., Bianchi, C., Bingham, R. G., Blankenship, D. D., Casassa, G., Catania, G., Callens, D., Conway, H., Cook, A. J., Corr, H. F. J., Damaske, D., Damm, V., Ferraccioli, F., Forsberg, R., Fujita, S., Gim, Y., Gogineni, P., Griggs, J. A., Hindmarsh, R. C. A., Holmlund, P., Holt, J. W., Jacobel, R. W., Jenkins, A., Jokat, W., Jordan, T., King, E. C., Kohler, J., Krabill, W., Riger-Kusk, M., Langley, K. A., Leitchenkov, G., Leuschen, C., Luyendyk, B. P., Matsuoka, K., Mouginot, J., Nitsche, F. O., Nogi, Y., Nost, O. A., Popov, S. V., Rignot, E., Rippin, D. M., Rivera, A., Roberts, J., Ross, N., Siegert, M. J., Smith, A. M., Steinhage, D., Studinger, M., Sun, B., Tinto, B. K., Welch, B. C., Wilson, D., Young, D. A., Xiangbin, C., and Zirizzotti, A.: Bedmap2: improved ice bed, surface and thickness datasets for Antarctica, The Cryosphere, 7, 375–393, doi:10.5194/tc-7-375- 2013, 2013

Griffies, S. M., Danabasoglu, G., Durack, P. J., Adcroft, A. J., Balaji, V., Böning, C. W., Chassignet, E. P., Curchitser, E., Deshayes, J., Drange, H., Fox-Kemper, B., Gleckler, P. J., Gregory, J. M., Haak, H., Hallberg, R. W., Heimbach, P., Hewitt, H. T., Holland, D. M., Ilyina, T., Jungclaus, J. H., Komuro, Y., Krasting, J. P., Large, W. G., Marsland, S. J., Masina, S., McDougall, T. J., Nurser, A. J. G., Orr, J. C., Pirani, A., Qiao, F., Stouffer, R. J., Taylor, K. E., Treguier, A. M., Tsujino, H., Uotila, P., Valdivieso, M., Wang, Q., Winton, M., and Yeager, S. G.: OMIP contribution to CMIP6: experimental and diagnostic protocol for the physical component of the Ocean Model Intercomparison Project, Geosci. Model Dev., 9, 3231–3296, https://doi.org/10.5194/gmd-9-3231-2016, 2016.

Hallberg, R: Using a resolution function to regulate parameterizations of oceanic mesoscale eddy effects, Ocean Model., 72, 92–103, doi:10.1016/j.ocemod.2013.08.007, 2013.

IOC, IHO and BODC: Centenary Edition of the GEBCO Digital Atlas, published on CD-ROM on behalf of the Intergovernmental Oceanographic Commission and the International Hydrographic Organization as part of the General Bathymetric Chart of the Oceans, British Oceanographic Data Centre, Liverpool, UK, 2003.

Iovino, D., Masina, S., Storto, A., Cipollone, A., and Stepanov, V. N.: A 1/16° eddying simulation of the global NEMO sea-ice–ocean system, Geosci. Model Dev., 9, 2665–2684, https://doi.org/10.5194/gmd-9-2665-2016, 2016.

Large, W. G. and Yeager, S. G.: Diurnal to decadal global forcing for ocean and sea–ice models: The data sets and flux climatologies, NCAR Tech. Note, TN–460+ST(May), 105 pp., https://doi.org/10.5065/D6KK98Q6, 2004.

Locarnini, R. A., Mishonov, A. V., Antonov, J. I., Boyer, T. P., Garcia, H. E., Baranova, O. K., Zweng, M. M., Paver, C. R., Reagan, J. R., Johnson, D. R., Hamilton, M., Seidov, D., and Levitus, S.: World Ocean Atlas 2013, Volume 1, Temperature, https://doi.org/10.7289/V55X26VD, 2013.

Madec, G. and Imbard, M.: A global ocean mesh to overcome the North Pole singularity, Clim. Dynam., 12, 381–388, 1996.
Madec, G. and the NEMO team: Nemo ocean engine – version 3.4, Technical Report ISSN 1288–1619, No. 27, Pôle de modélisation, Institut Pierre-Simon Laplace (IPSL), France, 2016.

Rio, M.-H., S. Mulet, and N. Picot: Beyond GOCE for the ocean circulation estimate: Synergetic use of altimetry, gravimetry, and in situ data provides new insight into geostrophic and Ekman currents, Geophys. Res. Lett., 41, doi:10.1002/2014GL061773, 2014.

Tsujino, H., Urakawa, L. S., Griffies, S. M., Danabasoglu, G., Adcroft, A. J., Amaral, A. E., Arsouze, T., Bentsen, M., Bernardello, R., Böning, C. W., Bozec, A., Chassignet, E. P., Danilov, S., Dussin, R., Exarchou, E., Fogli, P. G., Fox-Kemper, B., Guo, C., Ilicak, M., Iovino, D., Kim, W. M., Koldunov, N., Lapin, V., Li, Y., Lin, P., Lindsay, K., Liu, H., Long, M. C., Komuro, Y., Marsland, S. J., Masina, S., Nummelin, A., Rieck, J. K., Ruprich-Robert, Y., Scheinert, M., Sicardi, V., Sidorenko, D., Suzuki, T., Tatebe, H., Wang, Q., Yeager, S. G., and Yu, Z.: Evaluation of global ocean–sea-ice model simulations based on the experimental protocols of the Ocean Model Intercomparison Project phase 2 (OMIP-2), Geosci. Model Dev., 13, 3643–3708, https://doi.org/10.5194/gmd-13-3643-2020, 2020.

Tsujino, H., Urakawa, S., Nakano, H., Small, R. J., Kim, W. M., Yeager, S. G., Danabasoglu, G., Suzuki, T., Bamber, J. L., Bentsen, M., Böning, C. W., Bozec, A., Chassignet, E. P., Curchitser, E., Boeira Dias, F., Durack, P. J., Griffies, S. M., Harada, Y., Ilicak, M., Josey, S. A., Kobayashi, C., Kobayashi, S., Komuro, Y., Large, W. G., Le Sommer, J., Marsland, S. J., Masina, S., Scheinert, M., Tomita, H., Valdivieso, M., and Yamazaki, D.: JRA-55 based surface dataset for driving ocean–sea-ice models (JRA55-do), Ocean Model., 130, 79–139, https://doi.org/10.1016/j.ocemod.2018.07.002, 2018.

U.S. Department of Commerce: 2-minute Gridded Global Relief Data (ETOPO2v2), National Oceanic and Atmospheric Administration, National Geophysical Data Center, doi:10.7289/V5J1012Q, 2006.

Zweng, M. M., Reagan, J. R., Antonov, J. I., Locarnini, R. A., Mishonov, A. V., Boyer, T. P., Garcia, H. E., Baranova, O. K., Johnson, D. R., Seidov, D., and Biddle, M. M.: World Ocean Atlas 2013, vol. 2, Salinity, edited by: Levitus, and Mishonov, A., NOAA Atlas NESDIS 74, 39 pp., 2013